EUROGRAPHICS 2008 / G. Drettakis and R. Scopigno
(Guest Editors)

Volume 27 (2008), Number 2

An Adaptive Contact Model for the Robust Simulation of Knots

Jonas Spillmann Matthias Teschner

Computer Graphics, University of Freiburg, Germany

Abstract

In this paper, we present an adaptive model for dynamically deforming hyper-elastic rods. In contrast to existing approaches, adaptively introduced control points are not governed by geometric subdivision rules. Instead, their states are determined by employing a non-linear energy-minimization approach. Since valid control points are computed instantaneously, post-stabilization schemes are avoided and the stability of the dynamic simulation is improved.
Due to inherently complex contact configurations, the simulation of knot tying using rods is a challenging task. In order to address this problem, we combine our adaptive model with a robust and accurate collision handling method for elastic rods. By employing our scheme, complex knot configurations can be simulated in a physically plausible way.

Categories and Subject Descriptors (according to ACM CCS): I.3.7 [Computer Graphics]: Three-Dimensional Graphics and Realism: Animation

Keywords: Deformation Modeling, Elastic Rods, Adaptive Resolution, Contact Handling, Knot Simulation

1. Introduction

Physically-based simulation of one-dimensional elastic objects (rods) is a challenging problem in the area of computer animation. Although elastic rods are related to deformable solids and thin shells, rods in contact are particularly difficult to simulate due to their negligible volume and potentially complex contact geometries.

Real-world elastic rods are characterized by continuous mass distributions and displacement fields. In contrast, spatially discretized models have a restricted number of degrees-of-freedom (DOF). In order to achieve optimal simulation results with a limited computation power, the DOFs should adapt to varying configurations. If e. g. rods are employed in knot-tying simulations, different parts of a rod undergo time-varying small and large deformations. Moreover, segments can be collision free, or they can be involved in settings with a large number of contacts.

Spatially adaptive discretizations can be realized in various ways. In case of a *geometric adaptation*, the DOFs are arranged according to the geometric configuration of a rod. DOFs are introduced in regions with high curvature and removed in regions with low curvature. This technique is employed in cloth simulation to avoid artifacts if cloth is draped over sharp edges [BMF05]. As an alternative to geometric adaptation, *mechanical adaptation* is governed by contacts or other interactions [LGCM05, GLM06].

Main results: We propose an adaptive simulation of elastic rods in contact. Our approach works with any discrete hyper-elastic deformation model, i. e. a deformation model that defines a (necessarily convex) strain energy function W from which a stress-strain relationship can be derived. Our approach unifies contact handling with a dynamic multiresolution technique. However, we do not pre-compute different resolutions. Instead, DOFs are arranged based on geometric and mechanical adaptation criteria. Further, in contrast to previous work, we do not employ a virtual node technique [SSIF07], but refine the DOFs and adapt the governing differential equations. The approach faces the following challenges:

- Elastic rods are characterized by stiff differential equations and large deformations that have to be handled. Thus, it is generally not optimal to place a new control point at the barycenter of a segment as proposed in pre-

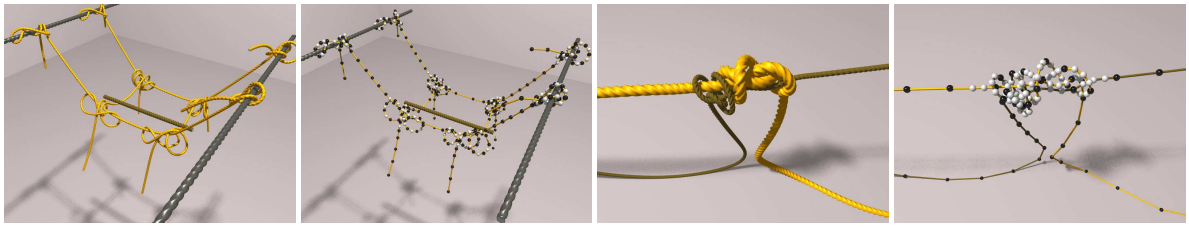

Figure 1: *In knot-tying simulations, large parts of the elastic rod are undeformed while a high mechanical accuracy is required to simulate the knot, which calls for adaptive methods. Left: A network linked by Prusik knots carries a bar element. The delicate equilibrium requires a robust collision handling method. Right: The double Fisherman's knot is used to tie together two ropes of unequal radii.*

vious works (e. g. [TWS06]). In contrast, we propose to determine the position of a new point as the root of a nonlinear system of equations in order to obtain a stable configuration. This novel technique could also be employed for adaptive cloth and body simulation.

- Due to the negligible volume of elastic rods, the discrete-time setting, and potentially complex contact configurations, penalty approaches and other local schemes are less appropriate to handle contacts. Thus, inspired by previous work on rigid and cloth collision handling [MS01, MHHR07], we propose an iterative scheme to solve a nonlinear system of non-penetration constraints.
- The dynamic refinement of the resolution causes discontinuous changes in the contact configuration. These discontinuities have to be considered by the contact handling method to guarantee a robust processing of contacts.

The proposed approach provides a stable and efficient simulation of virtual rods in contact. In combination with the CORDE deformation model [ST07], we show that complex tangled rods and knots can be simulated in a physically plausible way.

2. Related work

Contact handling. Little work exists that focuses on collision handling of elastic rods. Previous work includes the knot planning scheme of Saha et al. [SI06] and the dynamic knot-tying simulation of Brown et al. [BLM04] that shifts rope segments in a non-physical manner. Collisions occur frequently in hair simulation. Amongst others, Choe et al. [CCK05] and Bertails et al. [BKCN03, BAC*06] compute penalty forces based on interpenetrations. However, the volume of elastic rods is in general negligible compared to their longitudinal extent. Thus, a collision immediately results in an inconsistent state that comes along with the interpenetrations. In contrast to cloth collisions [BWK03, VMT06], such inconsistent states cannot be easily detected and resolved. Instead, collisions have to be avoided. Further, complex knots are characterized by a large number of simultaneous collisions that should be handled by a global response scheme. Such global schemes are widely used in rigid body collision response and result in a system of equations.

Usually, the problem of finding feasible impulsive or non-impulsive contact forces is formulated as a Linear Complementary Problem (LCP). Baraff published a variety of articles on how to compute contact forces that incorporate friction [Bar89, Bar91, Bar94]. LCP formulations have also been employed to resolve collisions of deformable volumetric objects [DDKA06] and quasi-rigid point clouds [PPG04]. However, solving an LCP is expensive, and the resulting solution is not necessarily more "correct" than other approaches, as pointed out by Kaufman et al. [KEP05]. They proposed to compute impulses by solving two separable Quadratic Programs (QP) per body. Non-penetration constraints can also be handled with Lagrange multipliers, as e. g. proposed by Galoppo et al. [GOM*06, GOT*07] in the context of deformable skin collision response. Other efficient alternatives have been proposed by Redon et al. [RKC02] and Bender et al. [BS06], where the latter proposes an iterative way to propagate impulses. The propagation of impulses can be accelerated by employing a contact graph, as shown by Guendelman et al. [GBF03].

Elastic rods have some resemblance with articulated rigid bodies [WTF06, GLM06], thin shells and cloth. In cloth collision response, most approaches assume rigid *impact zones* [Pro97] and solve for feasible velocities, either direct [HMB01] or in an iterative fashion [BFA02]. Similar to these approaches, we also compute impact zones, but drop the rigidity assumption since this would produce unrealistic behavior of knots.

Our approach shares similarities with a class of schemes that first compute feasible positions and then apply forces such that these positions are met after integration. Volino et al. [VMT00] employed a geometric scheme for computing positions, velocities and accelerations. Later, Milenkovic and Schmidl proposed a physically-based method for computing optimal configurations of rigid bodies [MS01] by solving a QP. And recently, Müller et al. presented a position-based simulation where non-penetration constraints are solved iteratively [MHHR07]. Our approach combines the accurate method of [MS01] with an efficient iterative scheme in the spirit of [GBF03] and [MHHR07] to compute feasible positions. Further, we ensure temporal coherence of the contact forces and consider that the mechanical adaptivity implies discontinuous changes in the contact state. In combination with the adaptive model, this results in an el-

egant and robust contact simulation of knotted threads and ropes.

Adaptive methods. To improve the efficiency and accuracy of deformable object simulation, adaptive methods reduce the DOFs in regions where mechanical or numerical accuracy is not mandatory. The refinement or reduction is governed by an error criterion which measures the adequacy of a given resolution. For three-dimensional meshes, this implies that either meshes at different resolutions are precomputed, or that the domain is remeshed. Since the latter is known to be a hard task, most works take the first approach. Debunne et al. [DDCB01] propose an adaptive simulation framework by employing finite element methods. At the interface, they interpolate the physical properties linearly between the nodes at different resolutions. By employing finite element methods, it is easier to guarantee that physical properties do not vary along different resolutions, which is in contrast to previous methods on adaptive mass-spring networks [HPH96]. Multi-resolution hexagonal grids allow for an efficient representation with octrees [BPWG07], and precomputed tetrahedral meshes can be avoided [CGC*02]. Recently, approaches that work with 'virtual particles' in order to adapt the resolution of a mesh gained increasing attention [EEHS00, SSIF07]. These approaches have proven to work well in practice although a plausible binding between virtual and real points can be difficult to realize.

For two-dimensional meshes that model e. g. thin shells, there exists a well-established theory of subdivision [ZS*99], which enables dynamic mesh refinement. An implementation of the multigrid scheme for thin shells is proposed by Green et al. [GTS02]. High-resolution meshes are particularly important for simulating folds and wrinkles in cloth. While geometric subdivision approaches such as [BFA02] aim at increasing the visual quality, Thomaszewski et al. [TWS06] propose a physically-based simulation of cloth where the elements are refined by employing Loop's scheme. Jain et al. [JKG*05] employ a multiresolution algorithm to speed-up collision detection. A different way is proposed by Grinspun et al. [GKS02]. Instead of refining the elements, they enlarge the approximation space by refining the basis functions. As a consequence, they avoid the compatibility problems at the interfaces between resolutions.

One-dimensional objects have an inherently simple topological structure that can be exploited by adaptive schemes. Pai proposed a physically-based deformation model for elastic rods that is based on the Cosserat theory [Pai02]. The rod is evolved by solving a boundary value problem. The step size can be chosen based on an adaptation criterion. Further, this model has the advantage that the control points are computed directly, analogous to a linear time dynamics algorithm for articulated rigid bodies. An adaptive method for snake-like articulated rigid bodies has been proposed by Gayle et al. [GLM06]. They rigidify joints in regions without collisions. And Bertails et al. [BKCN03] employed adaptivity in the context of hair clustering. They focus on control structures that approximate the large-scale coherent motion.

In our work, we focus on the adaptive simulation of discrete one-dimensional elastic objects. We start with a predefined mesh whose control points constitute the DOFs of the undeformed model. The mesh is then refined to meet the required accuracy. Lenoir et al. proposed an adaptive simulation of mechanical B-splines [LGCM05], where new control points are inserted based on geometric spline subdivision. However, for general elastic rod deformation models, it is not possible to compute the position of new control points analytically. By introducing the new control points at the barycenter of old control points, the potential energy is not minimized. In turn, the simulation becomes inevitably instable. To fight this problem, Phillips et al. [PLK02] proposed to add damping springs to the system after control point introduction. In contrast, we propose an adaptive simulation scheme that guarantees temporal coherence of the rod without employing any stabilization method. We show that the position of a refined node corresponds to the roots of a nonlinear system of equations.

3. Adaptive simulation overview

In this section, we briefly introduce the simulation loop for the constrained dynamic evolution of elastic rods. The subsequent sections explain the steps in detail. We employ the following simulation framework that has been previously proposed by e. g. [WTF06, DDKA06].

Simulation loop($\mathbf{g}^0$: initial configuration)
repeat
  deform: elastic forces of rod $\mathbf{g}^t$
  predict: integration results in unconstrained rod $\tilde{\mathbf{g}}^{t+h}$
  collision detection: detect interferences of $\tilde{\mathbf{g}}^{t+h}$
  collision response: compute contact forces
  correct: integration results in collision-free rod $\mathbf{g}^{t+h}$
  adapt: (un)refine rod based on adaptation criteria
until stop;

The key idea is to predict the unconstrained state of the rod at time $t+h$ by integrating the equations of motion, thereby neglecting contact forces. Then we detect interferences and compute contact forces that, if applied to the rod at time t, result in a interference-free state at $t+h$. Thus, difficulties related to post-stabilization techniques are avoided [WTF06].

In Sec. 4, we briefly describe the deformation model. The adaptive (un)refinement of the rod is discussed in Sec. 5. Collision detection and contact force computation are explained in Sec. 6, and the paper is concluded by presenting results in Sec. 7.

4. Deformation model

In this work, we assume that the deformation model for the rod is hyper-elastic. That means, there exists a scalar-valued strain energy density function $W(\mathbf{g}-\hat{\mathbf{g}})$, where $\mathbf{g}(\sigma,t)$: $\Omega\times\mathbb{R}\rightarrow\mathbb{R}^N$ is the configuration of the rod at time t defined on a domain $\Omega\subset\mathbb{R}$, and $\hat{\mathbf{g}}$ is the stress free resting configuration of the rod. The static equilibrium configuration is then

characterized as a critical point of the functional

$$\int_\Omega W(\mathbf{g}(\sigma) - \hat{\mathbf{g}}(\sigma))d\sigma - \int_\Omega \mathbf{g}(\sigma)\mathbf{F}d\sigma \qquad (1)$$

where $\mathbf{F}$ are generalized external forces. The dynamic equilibrium is obtained by considering the mass matrix and dissipation potentials. We require W to be convex, with a minimum at $W(\mathbf{0})$. Examples for such deformation models include the deformation models introduced by Phillips et al. [PLK02], Spillmann et al. [ST07], or Theetten et al. [TGAB07].

To numerically simulate the rod, a finite element method usually solves the weak form of the governing differential equation. The domain Ω is discretized into a disjoint union of $M-1$ elements. The nodes or *control points* $\mathbf{g}_i \in \mathbb{R}^N$ then comprise the DOFs of the elastic rod. For the CORDE deformation model, we e. g. have control points $\mathbf{g}_i = (\mathbf{r}_i^\mathsf{T}, \mathbf{q}_i^\mathsf{T})^\mathsf{T}$, with spatial control points $\mathbf{r}_i \in \mathbb{R}^3$ and quaternions $\mathbf{q}_i \in \mathbb{R}^4$. We collect the control points $\mathbf{g}_i$ in a control point vector $\mathbf{g} = (\mathbf{g}_1^\mathsf{T} \cdots \mathbf{g}_M^\mathsf{T})^\mathsf{T} \in \mathbb{R}^{MN}$, replacing the previously defined continuous configuration function $\mathbf{g}(\sigma)$. The resulting equations of motion are then

$$\mathbf{M}\ddot{\mathbf{g}} + \mathbf{d}(\dot{\mathbf{g}}, \mathbf{g}) + \mathbf{k}(\mathbf{g}) - \mathbf{F} = 0 \qquad (2)$$

with mass-matrix $\mathbf{M}$, dissipation function $\mathbf{d}$ and stiffness function $\mathbf{k}$.

5. Adaptive model

The simulation of knots requires a large number of DOFs in a small spatial region in order to meet the necessary mechanical accuracy. Still, large parts of the elastic rod stay undeformed and can be represented by employing only a few DOFs. That is why adaptivity is attractive in the simulation of elastic rods.

In this section, we present a solution for the adaptive simulation of rods. We work in the element point of view, i. e. we split or merge elements instead of basis functions [GKS02]. We first describe the adaptation criteria that govern the (un)refinement of the elements before focusing on the problem of node insertion and removal.

5.1. Adaptation criteria

Most existing adaptive schemes define adaptation criteria (sometimes also denoted as quality criteria or error criteria) solely on geometric properties, i. e. how well the basis functions approximate the current deformation state [DDCB01, CGC*02]. In multigrid approaches, one usually compares the solutions at different hierarchy levels [GTS02,OGRG07]. However, as Lenoir et al. [LGCM05] recognized, a pure geometric criterion is not sufficient for elastic rods. Instead, colliding elements have to be refined in order to meet the required DOFs. While Lenoir et al. only consider user interactions with the rod, we follow Gayle et al. [GLM06] who incorporate the contact configuration. More precisely, we bisect an element i if there is at least one contact on the left and on the right subelement. With this adaptation criterion, we can avoid the instabilities that are related to cascaded refinements. Two elements are merged if there has not been a contact for a user-defined time span t_{merge}.

We further define a geometric adaptation criterion that considers the local curvature of the rod, i. e. we refine the rod if the local curvature exceeds a user-defined threshold value. Similar to [DDCB01, LGCM05], we use a smaller threshold value to unrefine an element. In the experiments, we use a threshold value of 0.6 to refine and a threshold value of 0.2 to unrefine elements.

5.2. Element refinement

If the adaptation criteria for an element i are met, the element is bisected into two subelements i_1 and i_2, and a new control point $\mathbf{g}_i^+$ is introduced. Likewise, the element domain Ω_i is partitioned into disjoint subelement domains Ω_{i_1} and Ω_{i_2} with $\Omega_i = \Omega_{i_1} \cup \Omega_{i_2}$ in order to preserve the resting length of the rod. Previous approaches propose to place the introduced control point $\mathbf{g}_i^+$ at the barycenter of the old control points $\mathbf{g}_{i-1}^-$ and $\mathbf{g}_i^-$. However, since the curvature in the new control point $\mathbf{g}_i^+$ will be 0, the curvature energies are not distributed uniformly over the elements, which in turn causes instabilities in the underlying differential equations. While previous approaches recommend to add artificial damping springs to stabilize the simulation over time [PLK02], we propose a procedure that computes valid, i. e. energy-minimizing control points instantaneously.

Since a new control point cannot be inserted without either the stretch or the curvature varying discontinuously, the left or the right control point has to be displaced accordingly. For efficiency purposes, we always choose the neighboring control point whose adjacent line segments are involved in less collisions. The goal is to find new control point positions $\mathbf{g}_i^+$ and $\mathbf{g}_{i+1}^+$ such that the strain energy over the new elements is minimized (see Fig. 2). More precisely, the new positions $\mathbf{g}_i^+$ and $\mathbf{g}_{i+1}^+$ constitute the solution of the non-linear constrained minimization problem

$$\sum_{j=i-1}^{i+1} \int_{\Omega_j} W(\mathbf{g} - \hat{\mathbf{g}})d\sigma - \sum_{j=i}^{i+1} \mathbf{g}_j^\mathsf{T}\mathbf{F}_j \to \min \qquad (3)$$

subject to the holonomic boundary conditions

$$\mathbf{g}_{i-1}^+ - \mathbf{g}_{i-1}^- = 0 \qquad (4)$$

$$\mathbf{g}_{i+2}^+ - \mathbf{g}_{i+1}^- = 0 \qquad (5)$$

where the $\mathbf{F}_j$ are external forces such as gravity or contact forces acting on the control points. The incorporation of contact forces is important since displacing control points eventually result in interferences (see Sec. 6.6 for details). Intuitively, we seek the control points $\mathbf{g}_i^+$ and $\mathbf{g}_{i+1}^+$ that minimize the strain energy while preserving all other control points in the mesh (notice that $\mathbf{g}_{i+1}^-$ becomes $\mathbf{g}_{i+2}^+$ after refinement, as indicated in Fig. 2). Since the lengths of the new elements sum to the length of the old element, and since all other control points are fixed during refinement, both the current and the resting length of the rod are preserved.

The solution of this system of equations is computed by

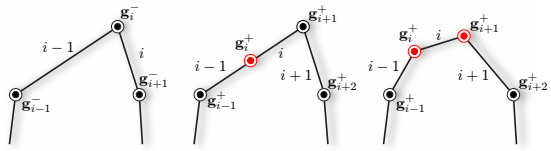

Figure 2: *By placing the new control point $\mathbf{g}_i^+$ at the barycenter of $\mathbf{g}_{i-1}^-$ and $\mathbf{g}_i^-$, the curvature changes discontinuously. In contrast, we compute energy-minimizing control points $\mathbf{g}_i^+$ and $\mathbf{g}_{i+1}^+$.*

a non-linear conjugate gradient (CG) method. The necessary analytic differentiation and integration of W is done with a symbolic computer algebra software. Notice that the gradient of W conforms to the restitution force vector. If analytic integration is not possible, the expressions can be obtained by a quadrature method. The step length for the line search in the CG algorithm is determined by employing the Wolfe conditions [NW99], with the initial guess depending on the employed deformation model (see Appendix). The conjugate direction parameter is computed with the Fletcher-Reeves formula. By only updating the coordinates of the control points $\mathbf{g}_i^+$ and $\mathbf{g}_{i+1}^+$ during minimization, we enforce the boundary conditions. Since we restrict W to be convex, the computed constrained minimum is guaranteed to be global. The necessary number of iterations depends on the deformation model. For moderately damped elastic rods simulated with CORDE, usually 5 to 10 iterations suffice to stabilize the simulation.

To preserve the dynamics of the rod, the mass-matrix $\mathbf{M}$ in (2) has to be updated. For approaches that assume mass-lumping, this conforms to recomputing the point-masses, which can be done efficiently. Further, the velocities of the new control points are linearly interpolated from the old control points.

5.3. Element unrefinement

To unrefine the rod, two neighboring elements are merged into one. Again, it is not possible to just remove a control point $\mathbf{g}_i^-$. Instead, either the left or the right control point has to be displaced to the energy-minimizing position. The solution of this non-linear minimization problem is similar to the refinement-case.

5.4. Remarks

The scheme in its present form always bisects elements in the middle. It is, however, easy to extend the scheme to general bisection rules. Moreover, since remeshing is trivial for one-dimensional structures, the scheme allows for both structured and unstructured refinement. Depending on the deformation model, it is necessary to enforce upper and lower bounds on the domains Ω_i, i. e. $\Omega_i \in [\Omega^{\min}, \Omega^{\max}]$. A mathematical analysis on these bounds is, however, beyond the scope of this paper.

The rods are skinned with a spline-interpolated tubical mesh. To avoid visible popping artifacts of the skin during refinement, we smoothly blend the old skin with the new skin. Thus, visual interferences might occur, especially in coarsely sampled regions with high curvature. We underline that this does not harm the mechanical accuracy since all physical operations are performed on the simulated mesh $\mathbf{g}$. Still, skinning is part of ongoing work.

6. Contact handling

In this section, we propose a novel approach for robust global contact handling of elastic rods. Together with the adaptive model, the approach allows for the accurate simulation of knots. After an unconstrained temporal evolution of the rods, we detect collisions in the (possibly) interfering state. We employ hierarchies of axis-aligned bounding boxes to detect collisions and self-collisions [TKH*05]. Similar to Müller [MHHR07], we impose non-penetration constraints on the primitives. We then seek for the minimum displacements that satisfy the constraints. By applying constraint forces, the rods meet the non-penetration constraints after evolution. Notice that since collisions are detected at discrete times, collisions can be missed in case of large relative velocities. However, this occurred very rarely in our experiments.

6.1. Constraint-based contact forces

In the following discussion, we assume that we can always extract spatial coordinates $\mathbf{r}_i \in \mathbb{R}^3$ from the generalized coordinates $\mathbf{g}_i$. The pair $S_i = (\mathbf{r}_i, \mathbf{r}_{i+1})$ constitutes a *segment* of the rod. Let

$$\mathrm{md}(i,j) = \mathrm{md}(\mathbf{r}_i, \mathbf{r}_{i+1}, \mathbf{r}_j, \mathbf{r}_{j+1}) > 0$$

be the minimum Euclidean distance between two rod segments S_i and S_j. Then the collision detection procedure provides a set of *collisions* (S_i, S_j), i. e. segments S_i and S_j for which $\mathrm{md}(i,j) < d$. Here, $d = r_i + r_j$ is the enforced minimum distance between the rod segments, with r_i and r_j the radii of the rods. The penetration depth $\varepsilon_{ij} > 0$ of a collision (S_i, S_j) is then $d - \mathrm{md}(i,j)$.

We define the contact space of a collision (S_i, S_j) to be spanned by the minimum distance vector $\mathbf{n}_{ij}$ between S_i and S_j. We are looking for displacements $\Delta\mathbf{r}_i$ such that the coordinates $\mathbf{r}_i + \Delta\mathbf{r}_i$ define an interference-free configuration. The displacement $\Delta\mathbf{r}_i$ is a linear combination

$$\Delta\mathbf{r}_i = \sum_{j \in \mathcal{C}(i)} \mathbf{n}_{ij} \chi_{ij} \tag{6}$$

with $\mathcal{C}(i)$ the set of all pairs of interfering segments that $\mathbf{r}_i$ is adjacent to, and unknown scalars χ_{ij}. The non-interference conditions for the set of collisions are written as

$$\begin{aligned} \mathrm{md}(\mathbf{r}_i + \Delta\mathbf{r}_i, \mathbf{r}_{i+1} + \Delta\mathbf{r}_{i+1}, \mathbf{r}_j + \Delta\mathbf{r}_j, \mathbf{r}_{j+1} + \Delta\mathbf{r}_{j+1}) &\geq d \\ \mathrm{md}(\mathbf{r}_k + \Delta\mathbf{r}_k, \mathbf{r}_{k+1} + \Delta\mathbf{r}_{k+1}, \mathbf{r}_l + \Delta\mathbf{r}_l, \mathbf{r}_{l+1} + \Delta\mathbf{r}_{l+1}) &\geq d \\ &\vdots \end{aligned} \tag{7}$$

As a second condition, the momentum must be conserved, i. e.

$$\sum_i \Delta \mathbf{r}_i m_i = 0 \tag{8}$$

According to Gauss' principle of least work (see e. g. [RKC02]), we are looking for the minimum displacements that result in an interference-free configuration, i. e. we require

$$\sum_i \|\Delta \mathbf{r}_i\|_2 \rightarrow \min \tag{9}$$

Together, these equations define a non-linear optimization problem. This formulation is similar to the optimization-based algorithm in [MS01] with the difference that we explicitly enforce the conservation of momentum.

6.2. Iterative solution

Computing the exact solution of the system of equations (7-9) is hardly feasible at interactive rates. Instead, we propose an iterative solution in the spirit of [GBF03, MHHR07] to obtain interference-free positions. We first group interacting collisions to *impact zones* (according to the definition of Provot [Pro97]). In contrast to [HMB01, BFA02], we do not treat these impact zones as rigid. We then solve for feasible positions for each collision individually: Let $\xi = \frac{m_j w_j + m_{j+1}(1-w_j)}{m_i w_i + m_{i+1}(1-w_i) + m_j w_j + m_{j+1}(1-w_j)}$ be the barycentrically weighted ratio of masses that accounts for conservation of momentum of the collision (S_i, S_j), with w_i being the barycentric coordinates of the contacts on the line segments. Notice that $\xi = \frac{1}{2}$ if all four points have same masses. Then the collision displacements

$$\begin{aligned} \Delta \mathbf{r}_i &= \mathbf{n}_{ij} \xi (\mathrm{md}(i,j) - d) w_i \\ \Delta \mathbf{r}_{i+1} &= \mathbf{n}_{ij} \xi (\mathrm{md}(i,j) - d)(1 - w_i) \\ \Delta \mathbf{r}_j &= \mathbf{n}_{ij} (1-\xi)(d - \mathrm{md}(i,j)) w_j \\ \Delta \mathbf{r}_{j+1} &= \mathbf{n}_{ij} (1-\xi)(d - \mathrm{md}(i,j))(1 - w_j) \end{aligned} \tag{10}$$

effect that the penetration depth ε_{ij} for this collision is at least halved, if the collision is considered in isolation. We account for spatial continuity by weighting the displacements with the barycentric coordinates of the collision. By processing all collisions per impact zone in a sequential manner, and summing the displacements per point $\mathbf{r}_i$, we obtain displacements that conserve the momentum (8). This process constitutes one step of the iterative scheme.

By repeating this process, displacements quickly propagate through the impact zone and secondary collisions are resolved (impact zones are merged if segments from different impact zones become colliding). The iterative search is stopped if $\varepsilon_{ij} < \varepsilon_{\max}$ for all collisions (S_i, S_j) in the impact zone, where $\varepsilon_{\max}$ is the error tolerance. Experiments indicate that the number of iterations depends linearly on the number of contacts, as expected. The number of iterations could be reduced by employing a contact graph, as proposed in [GBF03]. However, building a contact graph for knots is not straight-forward.

6.3. Friction

The incorporation of frictional forces complicates the problem. Still, friction is crucial for simulating knots. Analytical solutions approximate the friction by a friction cone [Bar91, DDKA06]. We propose a position-based approximative solution for frictional effects that is consistent with our iterative method. For each collision (S_i, S_j), we compute a Coulomb friction force component $\mathbf{F}^{\mathrm{fric}}$ orthogonal to the contact space. We then approximate the friction displacement $\Delta \mathbf{r}_i^{\mathrm{fric}}$ for the point $\mathbf{r}_i$ as $\Delta \mathbf{r}_i^{\mathrm{fric}} = \mathbf{F}^{\mathrm{fric}} w_i \frac{h^2}{m_i}$, where we assumed that the mass m_i is lumped in the points $\mathbf{r}_i$. Further, h is the time step. In each iteration and for each collision, we add the friction displacements to the collision displacements. We account for the exponential decrease of the collision displacements in the course of the iterative computation by weighting the friction displacements $\Delta \mathbf{r}_i^{\mathrm{fric}}$ with a factor $2^{-\mathrm{iter}}$, where *iter* denotes the current iteration. While this approximative friction produces plausible results at minor computational overhead, more elaborated models could eventually improve the accuracy and support perfect sticking.

6.4. Contact forces

Having computed the displacements $\Delta \mathbf{r}_i$ that yield feasible positions $\mathbf{r}_i + \Delta \mathbf{r}_i$, we compute a contact force that accelerates the mass points towards the feasible position. More precisely, we look for contact forces $\mathbf{F}_i$ that, if time-integrated numerically at time t, result in the feasible positions $\mathbf{r}_i^{t+h} = \mathbf{r}_i^t + \Delta \mathbf{r}_i$. Algebraic transformations lead to $\mathbf{F}_i = \frac{1}{h^2} \Delta \mathbf{r}_i m_i$. Similar formulations have been successfully applied for geometric constraint maintenance [GBT06], hair dynamics [CCK05] and deformable body collision response [SBT07]. Since this formulation considers the simulation time step, instabilities due to large contact forces are largely inhibited [SBT07].

The computed displacements and corresponding contact forces result in entirely inelastic collisions. This corresponds nicely to the fact that the textile material of ropes and threads is best modeled with inelastic collisions.

6.5. Contact handling in the element refinement

When the rod is refined, then control points $\mathbf{g}_i^+$ and $\mathbf{g}_{i+1}^+$ are displaced in order to minimize the elastic energy over the new elements (see Sec. 5). The iterative displacement of the control points in the CG method eventually results in secondary interferences, which in turn causes instabilities. We avoid these interferences by detecting collisions of the bisected elements in each CG iteration (which can be done efficiently since the potentially colliding elements are already known in advance). By considering the resulting contact force in the static equilibrium functional (3), interference-free control points are guaranteed.

7. Evaluation and applications

We have staged a series of experiments in order to evaluate our adaptive rod simulation. We exemplify our method by employing the CORDE deformation model [ST07]. We first show that our adaptive scheme preserves the dynamic behavior of the rod. We then investigate into the characteristics of the proposed collision response, and further present interactive applications. All experiments have been performed on an Intel Xeon PC, 3.8Ghz.

Adaptive model. One of the main benefits of the proposed adaptive model is that it determines the exact control point positions instantaneously. It does not assume time-coherence, i. e. by damping the control points over time as in previous approaches. Fig. 3 illustrates a collision of two angular accelerated rods with a rigid bar. While one rod has a fixed resolution, the other rod is refined to respond more accurately to the collision. As the images illustrate, the dynamic behavior of the refined rod does not significantly differ from the dynamics of the unrefined rod. In average, 10-20 CG iterations are necessary to obtain stable control point positions. The average time to insert or remove a control point is 1.5ms, which includes the time to update the data structures.

Elastic rods can be used to model threads or ropes in knot simulations. Here, large parts of the thread are undeformed while a high mechanical accuracy is required to represent the knot, therefore making an adaptive model particularly attractive. Fig. 4 illustrates a simulation of the shoelace knot. As the figure indicates, the sampling density in the knot and at the contact points with the poles is higher than in the undeformed parts. Black bullets indicate original control points while white bullets indicate dynamically inserted control points. In this challenging simulation, the user can interact with the thread. When the user unties the shoelace knot, the thread slips down, illustrating the effect of Coulomb friction.

To investigate the gain in efficiency when employing an adaptive model, we have simulated two ropes tied together with the double Fisherman's knot (see Fig. 5). We compare the behavior of an adaptive rope versus a uniformly sampled high-resolution rope whose sampling density conforms to the maximum resolution of the adaptive rod, and versus a uniformly sampled low-resolution rope whose sampling density conforms to the minimum resolution of the adaptive rope. For the adaptive rope, the allowed minimum element length is $\Omega_i^{\min} = \frac{1}{4}\Omega_i^0$ for all elements i. As a consequence, the maximum number of nodes for the adaptive rope (conforming to the number of nodes for the high-resolution rope) is four times the number of nodes of the low-resolution rope. As Tab. 1 indicates, simulating an adaptive rope is almost twice as efficient as the high-resolution rope. The number of collisions for both cases do not vary significantly, indicating that the adaptive rope does not result in a loss of accuracy. On the other hand, simulating the knot with a low-resolution rope results in physical and visual artifacts exhibited in Fig. 5. These artifacts are induced by the insufficient control point sampling.

For these moderately damped ropes, 10 iterations are sufficient to stabilize the simulation. If fewer iterations are performed, then the simulation becomes instable. The average time to (un-)refine the adaptive rope is 1.35ms. Still, since the adaptation criteria are only met in about 5% of all simulation steps, only 0.41% of the total simulation time is spent for node insertions and deletions.

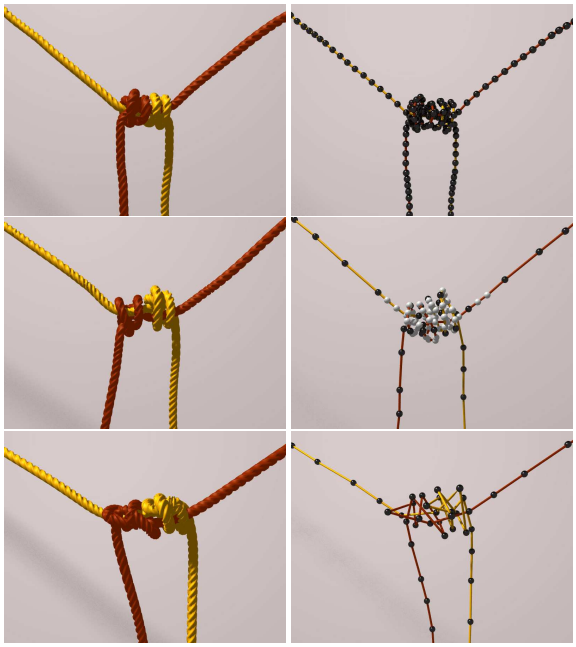

Figure 5: *Simulation of two ropes tied together with the double Fisherman's knot. Top: A high-resolution rope with 252 nodes. Middle: An adaptive rope with 116 nodes and the same maximum resolution as the high-resolution rope. Bottom: A low-resolution rope with 63 nodes.*

Employing an adaptive model always pays off in interactive knot-tying simulation when the location of the knot is not known in advance. Currently, the limiting factor for the refinement is the enforced minimum element length $\Omega^{\min}$, which depends on the deformation model and on the simulation parameters. A worst-case scenario for an adaptive rope is illustrated in Fig. 7, where most elements of the rope are involved in collisions. Thus the number of nodes of the adaptive rope conforms to the number of nodes of the high-resolution rope. Still, the simulation step timings for the adaptive and the high-resolution rope are about the same, illustrating that the overhead of the adaptivity is negligible.

Contact handling. Our physically motivated collision resolving scheme iteratively computes feasible collision-free positions of interfering rod elements. In each iteration, all contacts are processed to determine the locally feasible positions. Since displacing one rod element produces secondary collisions, the number of iterations depends linearly on the number of colliding elements. As a consequence, the complexity of the scheme is in $\mathcal{O}(n^2)$ with n the number of con-

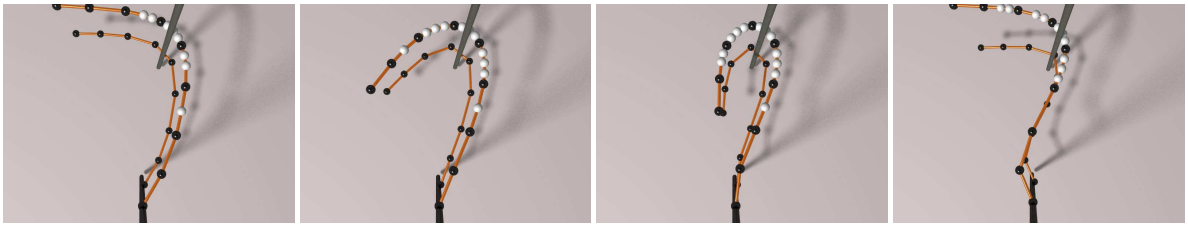

Figure 3: *Two rods with equal material properties are colliding with a rigid obstacle. One rod is dynamically refined while the other rod has a fixed resolution. The four images illustrate that the dynamic behavior is not affected by the refinement.*

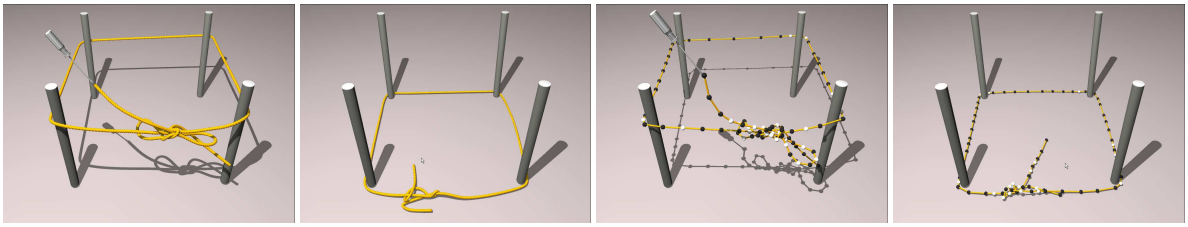

Figure 4: *Interactive simulation of adaptive knot-tying. A thread is tied around four poles, and a shoelace knot prevents it from slipping down. As the user unties the knot, the pressure is reduced and the thread slips to the ground. This simulation illustrates the effect of Coulomb friction.*

	High res.	Adaptive	Low res.
Nodes (Fig. 5)	252	(avg.) 116	63
Avg. collisions	70	69	22
Simulation step [ms]	13.3	7.3	2.6
Nodes (Fig. 7)	2K	(avg.) 1.9K	0.5K
Avg. collisions	10K	9.7K	2.6K
Simulation step [ms]	710	694	77

Table 1: *Statistics on the adaptive refinements. The upper three rows show the measurements of the simulation of the double Fisherman's knot (Fig. 5). As the measurements indicate, simulating the knot with adaptive ropes is almost twice as efficient and requires less than half the number of nodes than uniformly sampled ropes at the same maximum resolution. Still, the number of collisions does not vary significantly, illustrating that the knot is simulated with similar accuracy. In contrast, the low-resolution ropes cannot reproduce the knot configuration accurately enough. The lower three rows show the measurements of a worst-case scenario for adaptive ropes (Fig. 7), illustrating that the overhead for the adaptivity is negligible.*

tacts. Still, since computing locally feasible positions is a cheap operation, the running times are comparable to state-of-the-art response schemes. Fig. 6 relates the time to compute feasible positions to the number of contacts and underlines the theoretical result.

To show that we can resolve complex self-contact configurations, we ran a simulation of a falling coiled rope with 2K control points, as depicted in Fig. 7. The simulation time step

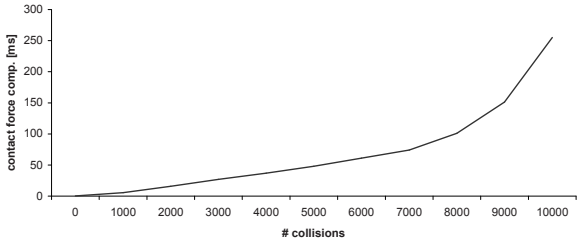

Figure 6: *The complexity of our global response scheme is in $\mathcal{O}(n^2)$. However, usually fewer than n iterations are necessary to resolve n collisions with sufficient accuracy. In the experiment, we have considered an error tolerance $\varepsilon_{max} = 10^{-3}r$, with r the radius of the rod.*

is 10^{-4}s. Collision detection of 10K collisions takes 355ms and computing feasible positions takes 255ms. The average initial penetration depth is $\varepsilon = 1.8 \cdot 10^{-3}r$, with r the radius of the rod. 34 iterations are necessary to reduce the penetration depth to $\varepsilon < \varepsilon_{\max} = 10^{-3}r$. Force computation and integration takes 100ms, the simulation runs at 1.5 frames per second.

8. Conclusion and future work

We have presented an adaptive model for hyper-elastic rods. Since the refinement of the rod should be governed by the contact configuration, our approach unifies adaptivity with robust collision handling. We have recognized that the stiff underlying differential equations do not allow to place new

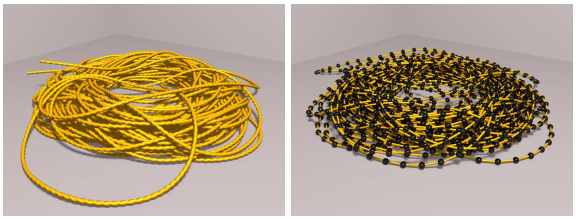

Figure 7: *Simulation of a coiled rope. The rope consists of 2K control points, with 10K collisions in average. This experiment illustrates global collision response in the context of massive self-collisions. Since most elements are involved in collisions, this simulation represents the worst-case scenario for adaptivity.*

control points based solely on geometric rules, as in previous approaches for cloth [TWS06] and deformable bodies [DDCB01]. In contrast, the control points result from an energy-minimization problem that is solved by employing a non-linear conjugate gradient method. In return, valid control points positions are found instantaneously, and no artificial damping is necessary to stabilize the system after refinement. As a consequence, the dynamic behavior of the elastic rod is not affected by the refinement, and the stability of the simulation is improved. The robust position-based contact handling method computes physically-plausible contact forces. Challenging knot simulations illustrate the benefits of the proposed method.

We detect and handle collisions and self-collisions at discrete time steps, which limits the allowed maximum relative velocity between rods. If the relative velocity exceeds this limit, then collisions can be missed. Currently, we are investigating into continuous collision handling methods. Moreover, since the collision handling is staged on a piecewise linear contact hull, rods tend to rattle if they slide on each other. Handling the collisions on a Cosserat contact hull would require to know the analytical curve. Still, the linear hull could be smoothed by employing e. g. spline curves.

Another issue that we have not convincingly solved is the skinning of the rods. Instead of employing spline-interpolated tubes, a more accurate skinning technique would be favorable. Moreover, a volume-preserving skin deformation [AS07] would further improve the realism.

References

[AS07] ANGELIDIS A., SINGH K.: Kinodynamic skinning using volume-preserving deformations. In *Proc. ACM SIGGRAPH/Eurographics Symposium on Computer Animation* (2007), pp. 129–140.

[BAC*06] BERTAILS F., AUDOLY B., CANI M.-P., QUERLEUX B., LEROY F., LÉVÊQUE J.: Super-helices for predicting the dynamics of natural hair. *ACM Transactions on Graphics 25*, 3 (2006), 1180–1187.

[Bar89] BARAFF D.: Analytical methods for dynamic simulation of nonpenetrating rigid bodies. In *Computer Graphics (Proc. SIGGRAPH)* (1989), vol. 23, pp. 223–232.

[Bar91] BARAFF D.: Coping with friction for non-penetrating rigid body simulation. In *Proc. Computer Graphics and Interactive Techniques* (1991), pp. 31–41.

[Bar94] BARAFF D.: Fast contact force computation for nonpenetrating rigid bodies. In *Proc. Computer Graphics and Interactive Techniques* (1994), pp. 23–34.

[BFA02] BRIDSON R., FEDKIW R., ANDERSON J.: Robust treatment of collisions, contact and friction for cloth animation. *ACM Transactions on Graphics* (2002), 594–603.

[BKCN03] BERTAILS F., KIM T.-Y., CANI M.-P., NEUMANN U.: Adaptive Wisp Tree: a multiresolution control structure for simulating dynamic clustering in hair motion. In *Proc. ACM SIGGRAPH/Eurographics Symposium on Computer Animation* (2003), pp. 207–213.

[BLM04] BROWN J., LATOMBE J.-C., MONTGOMERY K.: Real-time knot tying simulation. *The Visual Computer 20*, 2–3 (2004), 165–179.

[BMF05] BRIDSON R., MARINO S., FEDKIW R.: Simulation of clothing with folds and wrinkles. In *Proc. International Conference on Computer Graphics and Interactive Techniques* (2005), pp. 28–36.

[BPWG07] BOTSCH M., PAULY M., WICKE M., GROSS M.: Adaptive space deformations based on rigid cells. *Computer Graphics Forum 26*, 3 (2007), 339–347.

[BS06] BENDER J., SCHMITT A.: Constraint-based collision and contact handling using impulses. In *Proc. Computer Animation and Social Agents* (2006), pp. 3–11.

[BWK03] BARAFF D., WITKIN A., KASS M.: Untangling cloth. *ACM Transactions on Graphics 22*, 3 (2003), 862–870.

[CCK05] CHOE B., CHOI M., KO H.: Simulating complex hair with robust collision handling. In *Proc. ACM SIGGRAPH/Eurographics Symposium on Computer Animation* (2005), pp. 153–160.

[CGC*02] CAPELL S., GREEN S., CURLESS B., DUCHAMP T., POPOVIĆ Z.: A multiresolution framework for dynamic deformations. In *Proc. ACM SIGGRAPH/Eurographics Symposium on Computer Animation* (2002), pp. 41–47.

[DDCB01] DEBUNNE G., DESBRUN M., CANI M.-P., BARR A. H.: Dynamic real-time deformations using space and time adaptive sampling. In *Proc. SIGGRAPH* (2001), pp. 31–36.

[DDKA06] DURIEZ C., DUBOIS F., KHEDDAR A., ANDRIOT C.: Realistic haptic rendering of interacting deformable objects in virtual environments. *IEEE Transactions on Visualization and Computer Graphics 12*, 1 (2006), 36–47.

[EEHS00] ETZMUSS O., EBERHARDT B., HAUTH M., STRASSER W.: Collision adaptive particle systems. In *Proc. Pacific Graphics* (2000), pp. 338–347.

[GBF03] GUENDELMAN E., BRIDSON R., FEDKIW R.: Nonconvex rigid bodies with stacking. *ACM Transaction on Graphics 22*, 3 (2003), 871–878.

[GBT06] GISSLER M., BECKER M., TESCHNER M.: Local constraint methods for deformable objects. In *Third Workshop in Virtual Reality, Interactions and Physical Simulations* (2006), pp. 25–32.

[GKS02] GRINSPUN E., KRYSL P., SCHRÖDER P.: CHARMS: a simple framework for adaptive simulation. *ACM Transactions on Graphics 21*, 3 (2002), 281–290.

[GLM06] GAYLE R., LIN M., MANOCHA D.: Adaptive dynamics with efficient contact handling for articulated robots. In *Proc. of Robotics: Science and Systems* (2006).

[GOM*06] GALOPPO N., OTADUY M. A., MECKLENBURG P., GROSS M., LIN M. C.: Fast simulation of deformable models in contact using dynamic deformation textures. In *Proc. Eurographics/ACM SIGGRAPH Symposium on Computer Animation* (2006), pp. 73–82.

[GOT*07] GALOPPO N., OTADUY M. A., TEKIN S., GROSS M., LIN M. C.: Soft articulated characters with fast contact handling. *Computer Graphics Forum 26*, 3 (2007), 243–253.

[GTS02] GREEN S., TURKIYYAH G., STORTI D.: Subdivision-based multilevel methods for large scale engineering simulation of thin shells. In *Proc. ACM Symposium on Solid Modeling and Applications* (2002), pp. 265–272.

[HMB01] HUH S., METAXAS D., BADLER N.: Collision resolutions in cloth simulation. In *Proc. Computer Animation* (2001), pp. 122–127.

[HPH96] HUTCHINSON D., PRESTON M., HEWITT T.: Adaptive refinement for mass/spring simulations. In *Proc. 7th Eurographics Workshop on Animation and Simulation* (1996), pp. 31–45.

[JKG*05] JAIN N., KABUL I., GOVINDARAJU N., MANOCHA D., LIN M.: Multi-resolution collision handling for cloth-like simulations. *Computer Animation and Virtual Worlds* (2005), 141–151.

[KEP05] KAUFMAN D. M., EDMUNDS T., PAI D. K.: Fast frictional dynamics for rigid bodies. *ACM Transactions on Graphics 24*, 3 (2005), 946–956.

[LGCM05] LENOIR J., GRISONI L., CHAILLOU C., MESEURE P.: Adaptive resolution of 1D mechanical B-spline. In *Proc. Computer Graphics and Interactive Techniques in Australasia and South East Asia* (2005), pp. 395–403.

[MHHR07] MÜLLER M., HEIDELBERGER B., HENNIX M., RATCLIFF J.: Position based dynamics. *Journal of Visual Communication and Image Representation 18*, 2 (2007), 109–118.

[MS01] MILENKOVIC V., SCHMIDL H.: Optimization-based animation. In *Proc. Computer graphics and Interactive Techniques* (2001), pp. 37–46.

[NW99] NOCEDAL J., WRIGHT S.: *Numerical Optimization*. Springer Series in Operation Research, 1999.

[OGRG07] OTADUY M., GERMANN D., REDON S., GROSS M.: Adaptive deformations with fast tight bounds. In *Proc. ACM SIGGRAPH/Eurographics Symposium on Computer Animation* (2007), pp. 181–190.

[Pai02] PAI D.: STRANDS: Interactive Simulation of Thin Solids using Cosserat Models. *Computer Graphics Forum 21*, 3 (2002), 347–352.

[PLK02] PHILLIPS J., LADD A., KAVRAKI L. E.: Simulated knot tying. In *Proc. IEEE International Conference on Robotics & Automation* (2002), pp. 841–846.

[PPG04] PAULY M., PAI D. K., GUIBAS L. J.: Quasi-rigid objects in contact. In *Proc. Eurographics/ACM SIGGRAPH Symposium on Computer Animation* (2004), pp. 109–119.

[Pro97] PROVOT X.: Collision and self-collision handling in cloth model dedicated to design garments. *Graphics Interface 97* (1997), 177–189.

[RKC02] REDON S., KHEDDAR A., COQUILLART S.: Gauss'least constraints principle and rigid body simulations. *IEEE International Conference on Robotics and Automation 1* (2002), 517–522.

[SBT07] SPILLMANN J., BECKER M., TESCHNER M.: Non-iterative computation of contact forces for deformable objects. *Journal of WSCG 15*, 1-3 (2007), 33–40.

[SI06] SAHA M., ISTO P.: Motion planning for robotic manipulation of deformable linear objects. *Proc. IEEE International Conference on Robotics and Automation 27* (2006), 21–30.

[SSIF07] SIFAKIS E., SHINAR T., IRVING G., FEDKIW R.: Hybrid simulation of deformable solids. In *Proc. ACM SIGGRAPH/Eurographics Symposium on Computer Animation* (2007), pp. 81–90.

[ST07] SPILLMANN J., TESCHNER M.: CORDE: Cosserat rod elements for the dynamic simulation of one-dimensional elastic objects. In *Proc. ACM SIGGRAPH/Eurographics Symposium on Computer Animation* (2007), pp. 63–72.

[TGAB07] THEETTEN A., GRISONI L., ANDRIOT C., BARSKY B.: Geometrically exact dynamic splines. *Computer-Aided Design* (2007). to appear.

[TKH*05] TESCHNER M., KIMMERLE S., HEIDELBERGER B., ZACHMANN G., RAGHUPATHI L., FUHRMANN A., CANI M.-P., FAURE F., MAGNENAT-THALMANN N., STRASSER W., VOLINO P.: Collision Detection for Deformable Objects. *Computer Graphics Forum 24*, 1 (2005), 61–81.

[TWS06] THOMASZEWSKI B., WACKER M., STRASSER W.: A consistent bending model for cloth simulation with corotational subdivision finite elements. In *Proc. ACM SIGGRAPH/Eurographics Symposium on Computer Animation* (2006), pp. 107–116.

[VMT00] VOLINO P., MAGNENAT-THALMANN N.: Accurate collision response on polygonal meshes. In *Proc. Computer Animation* (2000), pp. 154–163.

[VMT06] VOLINO P., MAGNENAT-THALMANN N.: Resolving surface collisions through intersection contour minimization. In *ACM SIGGRAPH Papers* (2006), pp. 1154–1159.

[WTF06] WEINSTEIN R., TERAN J., FEDKIW R.: Dynamic simulation of articulated rigid bodies with contact and collision. *IEEE Transactions on Visualization and Computer Graphics 12*, 3 (2006), 365–374.

[ZS*99] ZORIN D., SCHRÖDER P., ET AL.: Subdivision for modeling and animation. *SIGGRAPH 99 Course Notes 2* (1999).

Appendix A: Finding energy-minimizing control points for CORDE rods

The CORDE deformation model [ST07] employs quaternions $\mathbf{q}_i$ to relate the local frame of an element i to the reference frame. The potential energy W is $W = V_s + V_b + E_p$, with V_s the stretching energy, V_b the bending energy, and E_p the constraint energy that aligns the local frames $\mathbf{q}_i$ with the tangent of the centerline. The initial configuration of the rods is user-defined, and the minimum element length $\Omega^{\min}$ depends on both the stiffness and the simulation time step.

Since the quaternion $\mathbf{q}_i$ corresponds to the direction of the element i, the number of unknowns in (3) is 18, notably two positions $\mathbf{r}_i$ and $\mathbf{r}_{i+1} \in \mathbb{R}^3$, and three quaternions $\mathbf{q}_{i-1}$, $\mathbf{q}_i$ and $\mathbf{q}_{i+1} \in \mathbb{R}^4$. The boundary conditions are $\mathbf{r}^+_{i-1} - \mathbf{r}^-_{i-1} = 0$, $\mathbf{r}^+_{i+2} - \mathbf{r}^-_{i+1} = 0$, $\mathbf{q}^+_{j-2} - \mathbf{q}^-_{j-2} = 0$ and $\mathbf{q}^+_{j+2} - \mathbf{q}^-_{j+1} = 0$.

The initial guesses for the step sizes in the non-linear CG algorithm are $\alpha_0^{(\mathbf{r})} = h^2 m_i^{-1}$ for the mass-points $\mathbf{r}_i$ and $\alpha_0^{(\mathbf{q})} = h^2 \mathrm{trace}(\mathbf{I})^{-1}$ for the quaternions $\mathbf{q}_i$, with h the simulation time step, and $\mathbf{I}$ the inertia tensor. Intuitively, these guesses guarantee convergence for the applied time step.